Analytical Estimation of the Propulsive Performance of Pulse Detonation Engines

Takuma Endo, Tomoaki Yatsufusa and Shiro Taki*
Hiroshima University, 1-4-1 Kagamiyama, Higashi-Hiroshima 739-8527, Japan
*takuma@mec.hiroshima-u.ac.jp

Jiro Kasahara
University of Tsukuba, 1-1-1 Tennodai, Tsukuba 305-8573, Japan

Akiko Matsuo, Kazuaki Inaba and Shigeru Sato
Keio University, Hiyoshi 3-14-1, Kohoku-ku, Yokohama 223-8522, Japan

Keywords: Pulse Detonation Engine, Propulsive Performance, Analytical Estimation

Abstract

We analytically estimated the propulsive performance of pulse detonation engines (PDEs) in three cases, which were (1) a fully-fueled simplified PDE, (2) a partially-fueled simplified PDE, and (3) a PDE optimized as a system. The results of the model analyses in the cases of (1) and (2) were in good agreement with published experimental data which were obtained by using simplified PDEs. The comparison between the results of the analyses of simplified PDEs and those of optimized PDE systems showed that specific impulse would become higher by about 10-20% due to PDE-system optimization.

Introduction

A pulse detonation engine (PDE) is an internal combustion engine in which fuel is repetitively burned as self-sustained detonation waves[1]. Since a PDE is of simpler structure and of higher theoretical thermodynamic efficiency compared with a conventional gas turbine engine which is based on isobaric combustion, research and development for its practical application are being progressed in the world.

Most of the experimental studies of PDEs have been carried out by using simplified PDEs[2-7], where a simplified PDE is defined as a straight detonation tube with fixed cross section, one end of which is closed and another end is open, except for some experiments carried out by private companies. And together with such experimental studies, modeling studies for predicting the propulsive performances of PDEs have been progressed mainly on simplified PDEs.

We so far have developed spread-sheet models, which are suitable not for pocket calculators but for spread-sheet or data-analysis softwares on desk-top computers, for the propulsive performances of fully-fueled (F-F) simplified PDEs[8] and partially-fueled (P-F) simplified PDEs[9]. In this paper, we briefly describe overviews of the models we developed so far, and a thermodynamic analysis of a PDE optimized as a system. Also, we compare the results of these analyses with published experimental data and discuss the degree of performance improvement by the optimization of PDE systems.

Theory of a F-F Simplified PDE

We simplified a PDE as a straight tube with fixed cross section, one end of which was closed and another end was open, where the closed end was the thrust wall. We theoretically obtained pressure history at the thrust wall for the case that such a tube was fully filled with a detonable gas at rest, where the initial state of the detonable gas was characterized by the pressure p_1 and the sound speed a_1, and that a self-sustained detonation wave was initiated at the thrust wall.

Figure 1 shows a schematic space-time (x-t) diagram of characteristics in a simplified PDE. At the

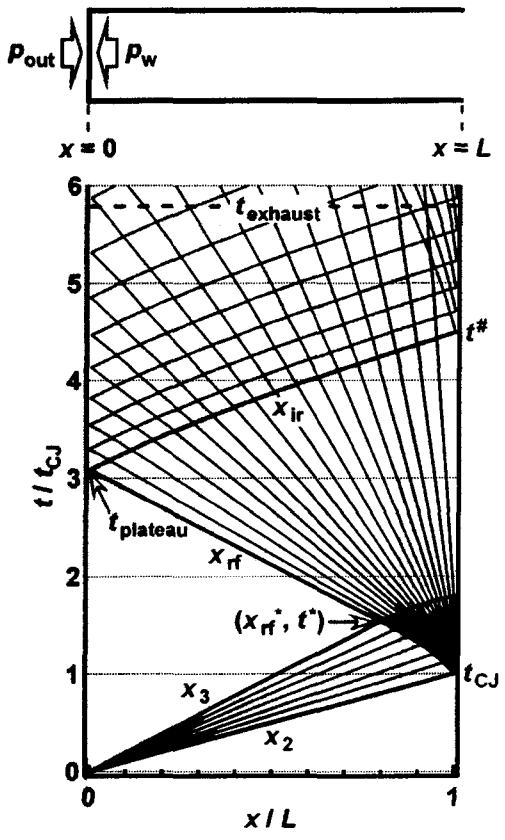

Fig. 1 Schematic space-time (x-t) diagram of characteristics in a simplified PDE.

time t=0 and the location x=0 (thrust wall), a self-sustained detonation wave is initiated. This detonation wave is regarded as a Chapman-Jouguet (CJ) detonation wave. In Fig. 1, x_2 denotes the position of the detonation wave, where the thickness of the detonation wave is neglected. A self-similar decelerating rarefaction wave (Taylor wave) follows the detonation wave. By this decelerating rarefaction wave, the boundary condition at the thrust wall, namely the condition that the gas is at rest at the thrust wall, is satisfied. In Fig. 1, the space region $x_3<x<x_2$ corresponds to this decelerating rarefaction wave. The detonation wave propagates from the closed end (x=0) toward the open end (x=L) with the propagation speed D_{CJ}, and reaches the open end at the time $t=t_{CJ}=L/D_{CJ}$. Since the flow in the rearward of the detonation wave is subsonic, an exhausting rarefaction wave starts to propagate from the open end toward the closed end at the time $t=t_{CJ}$. The front boundary of the exhausting rarefaction wave initially propagates in the decelerating rarefaction wave, and propagates in the gas at rest after the time $t=t^*$. In Fig. 1, x_{rf} denotes the position of the front boundary of the exhausting rarefaction wave. The front boundary of the exhausting rarefaction wave reaches the closed end at the time $t=t_{plateau}$. In the time region $0<t<t_{plateau}$, the pressure at the closed end is kept constant. After the time $t=t_{plateau}$, the exhausting rarefaction wave is reflected by the closed end, and the interference region between the exhausting rarefaction wave and its reflection extends from the closed end toward the open end. In Fig. 1, x_{ir} denotes the position of the boundary of this interference region. The boundary of this interference region reaches the open end at the time $t=t^{\#}$. Pressure at the thrust wall gradually decreases after the time $t=t_{plateau}$, and reaches the same value as the initial pressure p_1 at the time $t=t_{exhaust}$. At the time $t=t_{exhaust}$, the purge of the residual burned gas is started for the next cycle.

In order to formulate pressure history at the thrust wall in the above-mentioned process, we used some approximations. We regarded the unburned and burned gases as calorically perfect gases with the specific-heat ratios of γ_1 and γ_2, respectively. We assumed that viscosity and thermal-conduction effects were negligibly small. And we treated interference between the exhausting rarefaction wave and its reflection from the closed end as that between the self-similar rarefaction wave propagating from the open end toward the closed end in the uniform gas at rest and its reflection from the closed end. By using these approximations, we theoretically formulated the pressure history at the thrust wall as a function of time as

$$Function(p_w/p_1,\ t/t_{CJ};\ \gamma_1,\ \gamma_2,\ M_{CJ})=0, \qquad (1)$$

where p_w/p_1 is the pressure at the thrust wall normalized by the initial pressure, t/t_{CJ} is time normalized by the characteristic time t_{CJ}, and γ_1, γ_2 and $M_{CJ}=D_{CJ}/a_1$ are the governing parameters. In the time region $0<t<t_{plateau}$, the value of p_w/p_1 is given by a constant determined by γ_1, γ_2 and M_{CJ}. On the other hand, in the time region $t_{plateau}<t$, p_w/p_1 is given by an implicit function of time. Its functional form is not so simple as to calculate it with a pocket calculator.

Table 1 Parameters for the theoretical formula

Gas Mixture	γ_1	γ_2	M_{CJ}	D_{CJ}
H_2 + Air (stoichiometric)	1.394	1.167	4.852	1979
$2H_2+O_2$	1.396	1.129	5.276	2841
$C_2H_4+3O_2+N_2$	1.341	1.139	6.844	2269
$C_2H_4+3O_2$	1.329	1.140	7.267	2376
$C_2H_2+2.5O_2$	1.324	1.153	7.344	2425

(D_{CJ}: in m/s)

For calculation of the pressure history at the thrust wall, we have to know the parameters γ_1, γ_2, M_{CJ}, D_{CJ}, p_1 and L. The parameters p_1 and L are usually explicitly given. And also the initial temperature T_1 is usually explicitly given. Once p_1 and T_1 are given, the other parameters γ_1, γ_2, M_{CJ} and D_{CJ} can be determined by calculations based on the hydrodynamic conservation laws and chemical equilibrium. Table 1 shows examples of these parameters, which were calculated by using STANJAN[10] for the initial state that p_1=1 atm and T_1=300 K for comparison between the results of the theory and published experimental data. In these calculations, γ_1 and γ_2 were determined from frozen sound speed at the initial state and from equilibrium sound speed at the CJ point, respectively, by using the relation $\gamma=a^2\rho/p$, where ρ is the mass density. And we treated the air as the gas mixture written as O_2+3.76N_2.

Figure 2 shows the comparison between the theory and experiments[4] on the pressure history at the thrust wall. The detonable gas mixture was C_2H_4+3O_2, and it was initially at ambient conditions of pressure

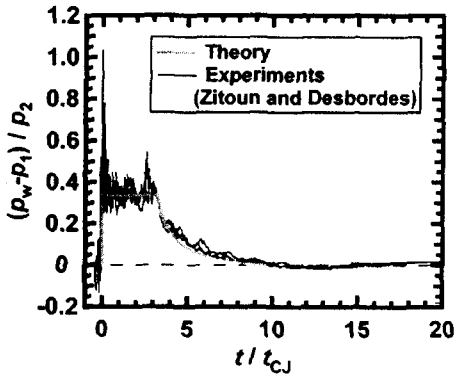

Fig. 2 Comparison between the theory and experiments on the pressure history at the thrust wall.

Table 2 Comparison between the theory and experiments on the specific impulse

Gas Mixture	Initiation	Frequency	Experiment [s]	Theory [s]	Ref.
$H_2 + Air$ (stoichiometric)	spark plugs & Shchelkin spiral	16 Hz	$I_{spf} = 3800 \sim 4450$	$I_{spf} = 4215$	(5)
$2H_2 + O_2$	spark plug only	single pulse	$I_{sp} = 191$	$I_{sp} = 186.3$	(6)
$C_2H_4 + 3O_2 + N_2$	spark plug only	single pulse	$I_{sp} = 159$	$I_{sp} = 160.8$	(6,7)
$C_2H_4 + 3O_2$	spark plug only	single pulse	$I_{sp} = 171$	$I_{sp} = 171.2$	(6,7)
$C_2H_2 + 2.5O_2$	spark plug only	single pulse	$I_{sp} = 202$	$I_{sp} = 172.7$	(6)
$C_2H_2 + 2.5O_2$	initiating tube	single pulse	$I_{sp} = 193 \sim 203$	$I_{sp} = 172.7$	(3)

and temperature. In Fig. 2, p_2 denotes the pressure at the CJ point. As shown in Fig. 2, the theoretical result was in good agreement with the experimental results. On specific impulse, Table 2 shows the comparison between the theory and experiments, where I_{sp} and I_{spf} denote mixture-based and fuel-based specific impulses, respectively. Except for the case of C_2H_2+2.5O_2, the theoretical results agreed with the experimental results within a few %. In the case of C_2H_2+2.5O_2, the theoretical result was lower than the experimental results by 12-18%. A probable reason of this disagreement may be the impurity of the detonable gas mixture because the obtaining of high-purity acetylene is generally not so easy.

Model of a P-F Simplified PDE

A P-F simplified PDE is schematically shown in Fig. 3(a). That is, a detonable gas occupies only a part of a detonation tube, and the other part of the tube is occupied by an inert gas. In Fig. 3, μ, u, ϕ_f, and Φ are the molar mass of a gas, flow velocity, the mass fraction of fuel in the detonable gas, and the mole fraction of the detonable gas in the all gases, respectively. By considering the boundary conditions at the closed end and at the interface between the detonable and inert gases, we assumed that

(a) Partially-Fueled PDE

Detonable Gas (Φ)	Inert Gas (1-Φ)
$p_{1,D}$, $a_{1,D}$, $\gamma_{1,D}$, $\gamma_{2,D}$,	$p_{1,I}$, $a_{1,I}$, γ_I,
$\mu_{1,D}$, $u_{1,D}$, $M_{CJ,D}$, $\phi_{f,D}$	μ_I, $u_{1,I}$

(b) Homogeneous-Dilution Model

Hypothetical Homogeneously-Diluted Detonable Gas
p_1, a_1, γ_1, γ_2, μ_1, u_1, M_{CJ}, ϕ_f

Fig. 3 Specifications of (a) the objective partially-fueled PDE and (b) the equivalent fully-fueled PDE.

$u_{1,I} = u_{1,D} = 0$ and $p_{1,I} = p_{1,D}$. Such partial fueling is known as a technique to make specific impulse higher[5].

In order to develop a model for estimating the propulsive performances of a P-F simplified PDE, we paid attention to the experimental fact[3] that the impulse of a simplified PDE hardly depended on the location of detonation initiation. Based on this experimental fact, we made a hypothesis that performance parameters of a simplified PDE which are obtained by integrating phenomena in one cycle are predominantly determined by energetics only. As a model based on this hypothesis, we proposed the homogeneous-dilution model shown in Fig. 3(b). In the homogeneous-dilution model, the objective P-F PDE is replaced with the equivalent F-F PDE which is defined so that it is fully filled with the homogeneous mixture of the detonable and inert gases with which the objective P-F PDE is filled. And after this replacement, the propulsive performances of the equivalent F-F PDE are estimated by using the theoretical formulas derived for F-F PDEs described in the preceding section.

Figure 4 shows the comparison between the homogeneous-dilution model and experiments[5]. In Fig. 4, I_{cyc} is the impulse per unit cross section per one cycle. The detonable gas was the stoichiometric hydrogen-air gas mixture, the inert gas was the air, and they were initially at ambient conditions of pressure and temperature. In the model, we used γ=7/5 for the specific-heat ratio of the air. The experimental dependence of the propulsive performance on the fueling fraction was well reproduced by the homogeneous-dilution model.

Thermodynamic Analysis of a PDE System

The degree of the improvement of PDE performances due to system optimization is a very important issue. In order to deal with this issue, we thermodynamically analyzed an open system shown in Fig. 5. This system includes a cyclic flow whose period is τ. In Fig. 5, m_{cyc}, Q_{cyc} and L_{cyc} are the mass of the gas flowing into or out from the system, the

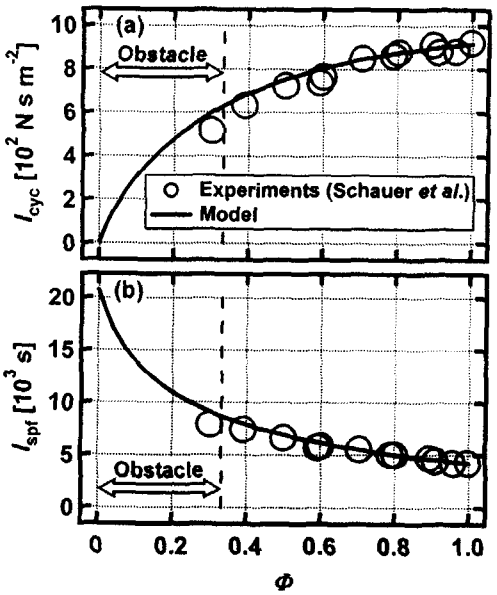

Fig. 4 Dependence of the propulsive performance on the fueling fraction.
(a) Impulse per unit cross section per one cycle.
(b) Fuel-based specific impulse.

heat released by combustion, and the work done to the outside of the system, respectively, during the period τ.

We applied the first law of thermodynamics to the control volume shown in Fig. 5, where viscosity and thermal-conduction effects were neglected. And integrating the obtained equation with respect to time over the period τ, we obtained the following equation:

$$Q_{cyc} - m_{cyc}\left(\overline{h_{outlet}} - \overline{h_{inlet}}\right) = L_{cyc} + m_{cyc}\left(\frac{\overline{u_{outlet}^2}}{2} - \frac{\overline{u_{inlet}^2}}{2}\right), \quad (2)$$

where the subscripts 'inlet' and 'outlet' denote the inlet and outlet of the system, respectively, $\overline{\ }$ denotes the mass-based average concerning all gases flowing into the system during the period τ, and h is the enthalpy of gas per unit mass. Defining theoretical thermodynamic efficiency η_{th0} by

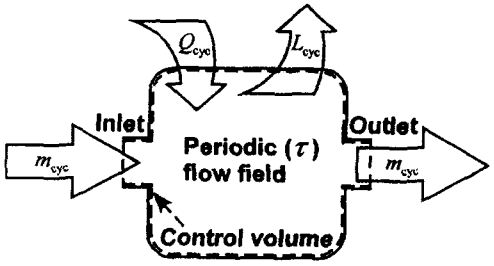

Fig. 5 PDE system as an open system.

$$\eta_{th0} = \frac{L_{cyc} + m_{cyc}\left(\frac{\overline{u_{outlet}^2}}{2} - \frac{\overline{u_{inlet}^2}}{2}\right)}{Q_{cyc}}, \quad (3)$$

we obtained the following formula:

$$\eta_{th0} = \frac{\bar{q} - \left(\overline{h_{outlet}} - \overline{h_{inlet}}\right)}{\bar{q}}, \quad (4)$$

where q is the heat released by combustion per unit mass of the gas. A detonable gas and an inert gas flow into the system during one cycle. Therefore, if the species and molar ratio of these gases are determined, $\bar{q}$ can be calculated. And if the processes experienced by the detonable and inert gases are determined, $\overline{h_{inlet}}$ and $\overline{h_{outlet}}$ can be calculated, and finally we can calculate the theoretical thermodynamic efficiency η_{th0}.

In the case of PDE systems, the detonable gas experiences the following process:
inflow state denoted by the subscript 'inlet'
→ adiabatic (isentropic) compression
→ pre-combustion state denoted by the subscript 1
→ combustion as the CJ detonation wave
→ post-combustion state denoted by the subscript 2
→ adiabatic (isentropic) expansion
→ outflow state denoted by the subscript 'outlet',
and the inert gas experiences the following process:
inflow state denoted by the subscript 'inlet'
→ adiabatic (isentropic) compression
→ pre-shock-compression state denoted by the subscript 1
→ shock compression (because the inert gas is contiguous to the detonable gas)
→ post-shock-compression state denoted by the subscript 2
→ adiabatic (isentropic) expansion
→ outflow state denoted by the subscript 'outlet'.

Furthermore, for estimating the propulsive performances of optimized PDE systems, I_{cyc} and I_{spf}, we assumed the following.

$$u_{outlet,D} = u_{outlet,I} = u_{outlet}, \quad (5)$$

$$p_{inlet,D} = p_{inlet,I} = p_{inlet}, \quad (6)$$

$$p_{outlet,D} = p_{outlet,I} = p_{outlet}, \quad (7)$$

and

$$L_{cyc} \ll m_{cyc}\left(\frac{u_{outlet}^2}{2} - \frac{u_{inlet}^2}{2}\right), \quad (8)$$

where the subscripts 'D' and 'I' denote the detonable and inert gases, respectively. By using these assumptions, we obtained the following formulas.

$$u_{\text{outlet}} = \sqrt{2\bar{q}\eta_{\text{th}0} + u_{\text{inlet}}^{\ 2}}, \tag{9}$$

$$I_{\text{cyc}} = m_{\text{cyc,D}} \left[\begin{array}{l} (1+\lambda)(u_{\text{outlet}} - u_{\text{inlet}}) \\ +(p_{\text{outlet}} - p_{\text{inlet}}) \dfrac{v_{\text{outlet,D}} + \lambda v_{\text{outlet,I}}}{u_{\text{outlet}}} \end{array} \right], \tag{10}$$

and

$$I_{\text{spf}} = \frac{1}{\phi_{\text{f}} g} \left[\begin{array}{l} (1+\lambda)(u_{\text{outlet}} - u_{\text{inlet}}) \\ +(p_{\text{outlet}} - p_{\text{inlet}}) \dfrac{v_{\text{outlet,D}} + \lambda v_{\text{outlet,I}}}{u_{\text{outlet}}} \end{array} \right], \tag{11}$$

where

$$\lambda = \frac{m_{\text{cyc,I}}}{m_{\text{cyc,D}}} = \frac{\mu_{\text{I}}}{\mu_{\text{D}}} \left(\frac{1}{\Phi} - 1 \right), \tag{12}$$

v and g are the specific volume and the standard sea-level value of gravitational acceleration, respectively.

Figure 6 shows the comparison among the results of the above-described thermodynamic analysis of a PDE system, the model analysis of a simplified PDE, and experiments[5] in which a simplified PDE was used. The detonable gas was the stoichiometric hydrogen-air gas mixture, the inert gas was the air, and they were initially at ambient conditions of pressure and temperature. In the thermodynamic analysis, we assumed that $u_{\text{inlet}}=0$ and $p_1/p_{\text{inlet}}=1$.

Figure 6(a) shows the dependence of I_{spf} on $p_{\text{outlet}}/p_{\text{inlet}}$ in the case of the F-F PDE ($\Phi=1$). We varied the parameter $p_{\text{outlet}}/p_{\text{inlet}}$ only within the condition that the outflow velocity was not subsonic. Whereas $I_{\text{spf}} = 3800 \sim 4450$ s experimentally and $I_{\text{spf}} = 4215$ s by the theoretical analysis on a F-F simplified PDE, the thermodynamic analysis showed that I_{spf} was the highest of $I_{\text{spf}} = 5037$ s when $p_{\text{outlet}}/p_{\text{inlet}}=1$. That is, this comparison shows that we could make I_{spf} higher by about 20% than a simplified PDE by optimizing a PDE system. Whether 20%-higher I_{spf} is significant or not is an issue to which we should give careful consideration taking account of mass increase due to the PDE-system optimization.

Figure 6(b) shows the dependence of I_{spf} on Φ. In the thermodynamic analysis, we assumed that $p_{\text{outlet}}/p_{\text{inlet}}=1$, and also $p_{2,\text{I}}/p_{1,\text{I}}=1$, namely, we neglected the shock compression of the inert gas. When the specific-heat ratio of the inert gas is assumed to be constant, the assumption of $p_{2,\text{I}}/p_{1,\text{I}}=1$ tends to result in overestimation of I_{spf}. That is, the results of the thermodynamic analysis shown in Fig. 6(b) may be regarded as the upper limits of I_{spf} of the optimized PDE systems. Figure 6(b) shows that in the case of P-F PDEs ($\Phi<1$), we could make I_{spf} higher by about 10-20% than a simplified PDE by optimizing a PDE system.

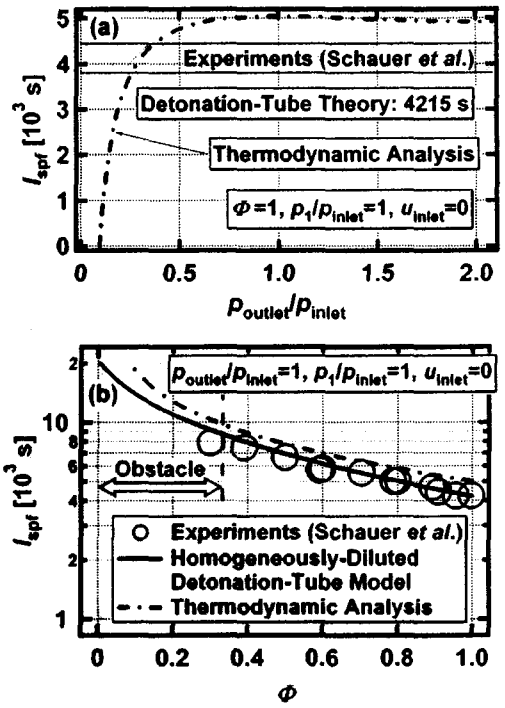

Fig. 6 Comparison among the thermodynamic analysis, the detonation-tube model, and experiments on the propulsive performance.
(a) Exhaust-pressure dependence.
(b) Fueling-fraction dependence.

Summary

We developed models for estimating the propulsive performances of simplified PDEs. On the specific impulse of simplified PDEs, the developed models reproduced published experimental data very well. In order to estimate the degree of performance improvement by the optimization of PDE systems, we thermodynamically analyzed a simple open system which included periodic flow field. The comparison between the experimental results obtained with simplified PDEs and the results of the thermodynamic analysis of an optimized PDE system showed that we could make the specific impulse higher by about 10-20% than a simplified PDE by optimizing a PDE system. Whether 10-20%-higher specific impulse is significant or not is an issue to which we should give careful consideration taking account of mass increase due to the PDE-system optimization.

Acknowledgments

The organization of this joint research was supported by Hokkaido Technology Licensing Office Co. Ltd. This work was financially supported by Regional Research & Development Consortium Project from Hokkaido Bureau of Economy, Trade and Industry.

References

1) Kailasanath, K., "Review of Propulsion Applications of Detonation Waves," *AIAA Journal*, Vol. 38, No. 9, 2000, pp. 1698-1708.
2) Nicholls, J. A., Wilkinson, H. R., and Morrison, R. B., "Intermittent Detonation as a Thrust-Producing Mechanism," *Jet Propulsion*, Vol. 27, No. 5, 1957, pp. 534-541.
3) Zhdan, S. A., Mitrofanov, V. V., and Sychev, A. I., "Reactive Impulse from the Explosion of a Gas Mixture in a Semi-infinite Space", *Combustion, Explosion, and Shock Waves*, Vol. 30, No. 5, 1994, pp. 657-663.
4) Zitoun, R. and Desbordes, D., "Propulsive Performances of Pulsed Detonations," *Combustion Science and Technology*, Vol. 144, 1999, pp. 93-114.
5) Schauer, F., Stutrud, J., and Bradley, R., "Detonation Initiation Studies and Performance Results for Pulsed Detonation Engine Applications", AIAA Paper 2001-1129, Jan. 2001.
6) Wintenberger, E., Austin, J. M., Cooper, M., Jackson, S., and Shepherd, J. E., "Impulse of a Single-Pulse Detonation Tube", Graduate Aeronautical Labs., GALCIT Rept. FM00-8, California Inst. of Technology, Pasadena, CA, August 2002.
7) Cooper, M., Jackson, S., Austin, J., Wintenberger, E., and Shepherd, J. E., "Direct Experimental Impulse Measurements for Detonations and Deflagrations," *Journal of Propulsion and Power*, Vol. 18, No. 5, 2002, pp. 1033-1041.
8) Endo, T., Kasahara, J., Tanahashi, Y., Numata, T., Matsuo, A., Sato, S., and Fujiwara, T., "Pressure History at the Thrust Wall of a Simplified Pulse Detonation Engine," Proceedings of the 19th International Colloquium on the Dynamics of Explosions and Reactive Systems, Hakone, Japan, 2003, #35.
9) Endo, T., Yatsufusa, T., Taki, S., Kasahara, J., Matsuo, A., Sato, S. and Fujiwara, T., "Homogeneous-Dilution Model of Partially-Fueled Pulse Detonation Engines," AIAA Paper 2004-1214, Jan. 2004.
10) Reynolds, W. C., "The Element Potential Method for Chemical Equilibrium Analysis: Implementation in the Interactive Program STANJAN, Version 3," Technical Rept., Dept. of Mechanical Engineering, Stanford Univ., Stanford, CA, Jan. 1986.

Appendix

Nomenclature

a	sound speed
D_{CJ}	Chapman-Jouguet detonation speed
g	standard sea-level value of gravitational acceleration
h	enthalpy of gas per unit mass
I_{cyc}	impulse per unit cross section per one cycle
I_{sp}	mixture-based specific impulse
I_{spf}	fuel-based specific impulse
L	length of PDE tube
L_{cyc}	work done to outside of system during the period τ
M_{CJ}	propagation Mach number of Chapman-Jouguet detonation wave; $M_{CJ} = D_{CJ}/a_1$
m_{cyc}	mass of gas flowing into or out from system during the period τ
p	pressure
q	heat released by combustion per unit mass of gas
Q_{cyc}	heat released by combustion during the period τ
T	temperature
t	time relative to the instant of ignition
t^*	time at which $x_{rf}=x_3$
$t^\#$	time at which $x_{ir}=L$
t_{CJ}	time at which detonation wave reaches open end of PDE tube
$t_{exhaust}$	time at which $p_w=p_1$
$t_{plateau}$	time at which plateau of pressure history at thrust wall ends
u	flow velocity relative to PDE tube
v	specific volume; $v=1/\rho$
x	coordinate along with axis of PDE tube
x_{ir}	boundary of interference region between exhausting rarefaction wave and its reflection from closed end of PDE tube
x_{rf}	front boundary of exhausting rarefaction wave
x_{rf}^*	x_{rf} at the time t^*
Φ	initial mole fraction of detonable gas in partially-fueled PDE
ϕ_f	initial mass fraction of fuel in detonable gas
γ	ratio of specific heats at constant pressure and volume
η_{th0}	theoretical thermodynamic efficiency of PDE system
λ	mass ratio between inert and detonable gases
μ	molar mass
ρ	mass density
τ	period of cyclic PDE operation

Subscripts

1	front of detonation or shock wave
2	rear of detonation or shock wave
3	rear boundary of decelerating rarefaction wave
D	detonable gas in partially-fueled PDE

I	inert gas in partially-fueled PDE
inlet	inlet of PDE system
out	outer surface of thrust wall of PDE tube
outlet	outlet of PDE system
w	inner surface of thrust wall of PDE tube

Others

$\overline{}$ mass-based average concerning all gases flowing into the system during the period τ